NASA/CR-1998 208346

MAPPING THE SOLAR WIND FROM ITS SOURCE REGION INTO THE OUTER CORONA

NASA Grant NAG5-6192

Annual Report

For the period 1 August 1997 through 31 July 1998

Principal Investigator
Ruth Esser

June 1998

Prepared for
National Aeronautics and Space Administration
Washington, D.C. 20546

Smithsonian Institution
Astrophysical Observatory
Cambridge, Massachusetts 02138

The Smithsonian Astrophysical Observatory
is a member of the
Harvard-Smithsonian Center for Astrophysics

The NASA Technical Officer for this Grant is Dr. William J. Wagner, 078.0 Code SR, NASA Headquarters, Washington, DC 20546.

Mapping the Solar Wind from the Source Region into Interplanetary Space Annual Report for the Period August 1 1997 to July 31 1998

1. Summary

1.1 Scope of the Investigation

Knowledge of the radial variation of the plasma conditions in the coronal source region of the solar wind is essential to exploring coronal heating and solar wind acceleration mechanisms. The goal of the present proposal is to determine as many plasma parameters in that region as possible by coordinating different observational techniques, such as Interplanetary Scintillation Observations, spectral line intensity observations, polarization brightness measurements and X-ray observations. The inferred plasma parameters are then used to constrain solar wind models.

1.2 Progress Made

Over the past year we have concentrated on the information that can be gained from UVCS/SOHO spectral line observations. As before we have concentrated on polar coronal hole observations, but we have also started to make the comparison to the surrounding regions. Jointly with John Kohl and Silvano Fineschi from the UVCS team, we have carried out three observational series of UVCS spectral lines. These lines, in conjunction with other solar corona/solar wind observations were used to estimate physical properties of the coronal plasma. An example is shown in Figure 1.

Figure 1 (upper panel) shows a composite image of the corona in X-rays from YOHKOH, polarized brightness from HAO Mk III coronagraph (1-2 R_S) and white light intensity from SOHO/LASCO C2 coronagraph (2-6 R_S). The lower panels are examples of solar wind parameters inferred from the observations. The effective ion temperatures are from Esser et al. (1998a) and Kohl et al. (1997 and 1998). The middle panels show coronal densities derived from pB measurements in a polar coronal hole (Fisher and Guhathakurta 1995) and in a equatorial region (Saito 1970). Using constraints from in situ ULYSSES observations, we have calculated a number of plasma parameters, such as flow speeds and Alfvén speeds. Using the wealth of information available on polar coronal plasmas from previous spacecraft observations, and the new SOHO observations, we have derived limits on the Alfvén wave amplitudes for the first time out to distances of 3 R_S. We find that the limits on the amplitude at the coronal base fit well with previous observations, and that WKB assumption fits with the observational constraints. The limits on the Alfvén wave amplitude are shown in Figure 2 a. Als shown is the ratio $\delta B/B = \delta v/v_A$ which is a measure for the linearity/damping of the waves. Using the limits on the amplitudes from Figure 2a we have then calculated the limits on the particle temperatures (Figure 2b). A comparison to the electron temperature derived by modeling ion charge states with high outflow speeds is also shown (Esser et al. 1998a). Using the plasma parameters shown in Figures 1 and 2, we then calculated the solar wind expansion time as a function of radial distance (Figure 2c, dashed lines), and the collision times between the heavy ions and the protons. It was shown that even though collision times between Mg ions and protons are small compared to the expansion times at 1.35 R_S, the thermal temperatures of the two ion species are not the same at that distance. This indicates that the heating mechanism that heats the heavy ions, has to act on time scales short compared to the collision times in order to maintain the observed temperature differences. Figure 2c also shows that collisions in the inner corona are important and should not be neglected in coronal heating studies.

The temperatures shown in Figure 1 were also used in solar wind model studies. Figure 3 shows an example of a study of different heating mechanism (Li et al. 1998). In this study it is assumed that low frequency Alfvén waves heat the corona and accelerate the solar wind. The waves dissipate in the inner corona at the Kolmogorov rate, a mechanism originally suggested by Hollweg (1986), and the Kraichnan heating rate. The study involved a three-fluid (electron-proton-He^{++}) solar wind. Both mechanisms produce solar wind flows that satisfy current observational constraints. The upper panels show the observed electron densities in the inner corona (error bars) together with the calculated values (solid lines), and the corresponding flow speeds. The lower panels show the corresponding particle temperatures together with upper and lower observational constraints on the proton temperature. This example shows that it is not possible to distinguish observationally between the two different heating mechanisms. A more detailed plasma physics study is needed to work out the proper heating mechanism(s). This should also include a heating source for the electrons. It is clear from the above study that heat input to the ions alone, will not result in a sufficient heating of the electrons since the collisional coupling between the protons and electrons is not sufficient to increase the electron temperature to observed values. Thus an additional heating source for the electrons has to exist. Heating mechanisms presently discussed for coronal heating only address the ion heating, e.g. ion cyclotron resonance. The above example, and the estimated collisional coupling (Figure 2c) between protons and electrons suggest that the electrons have to be heated differently.

References

Esser, R. et al., 1998, *ApJ Let.*, in press.
Fisher, R. R. and Guhathakurta, M., *Ap J*, *447*, L139, 1995
Hollweg, J. V., *J. Geophys. Res.*, *91*, 4111, 1986.
Kohl, J. et al., 1998, *ApJ Let.*, in preparation.
Kohl, J. et al., 1987, *Sol. Phys.*, 175, 613.
Li, X. et al., 1998, in preparation.
Saito, K., *Ann. Tokyo Obs.*, Ser. 2, 12, 53, 1970.

Figure 1: *The upper panel shows a composite image of the corona in X-rays from YOHKOH, polarized brightness from HAO Mk III coronagraph (1-2 R_S) and white light intensity from SOHO/LASCO C2 coronagraph (2-6 R_S). Effective temperatures, T_{eff}, derived from UVCS measurements.*

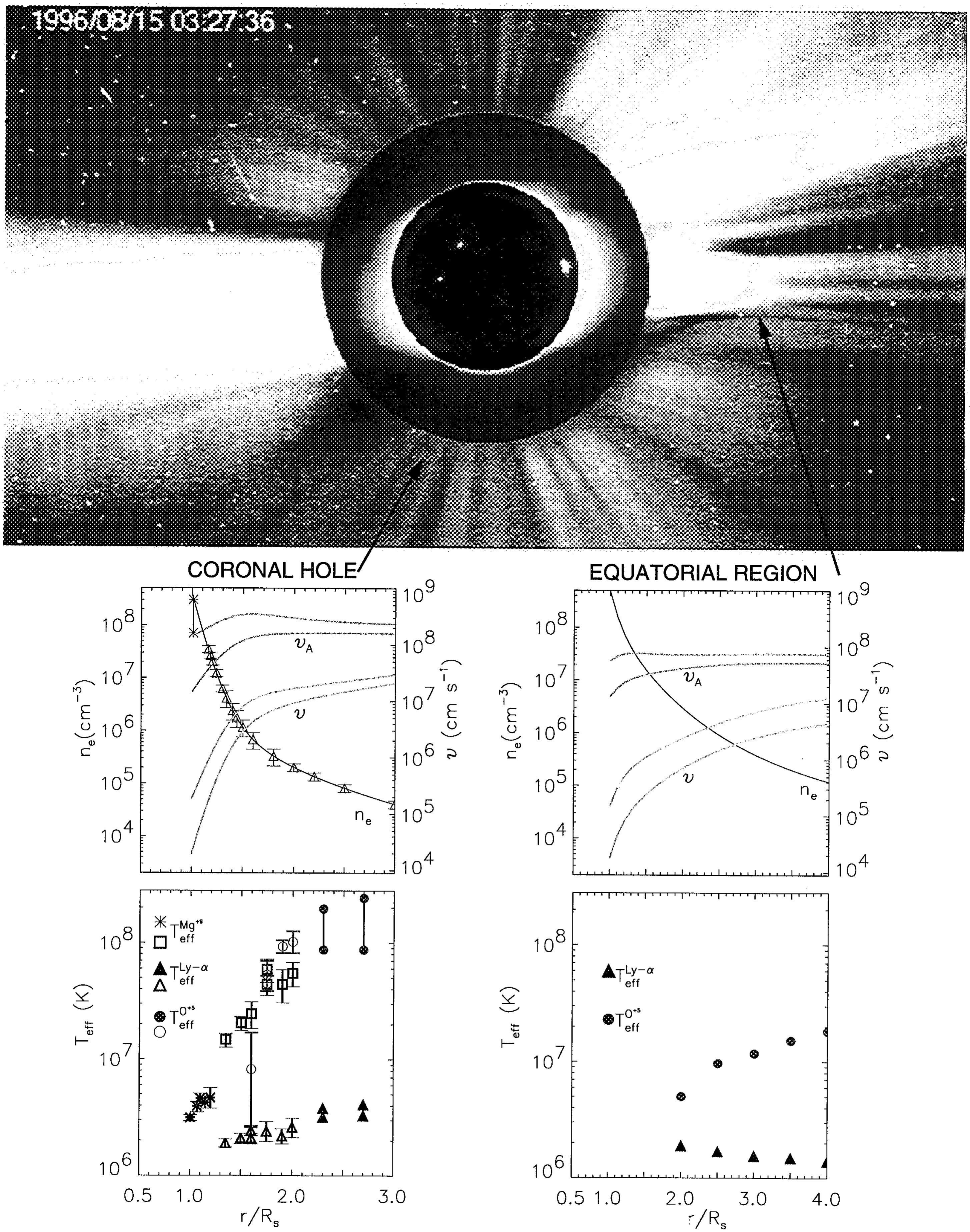
1996/08/15 03:27:36
CORONAL HOLE
EQUATORIAL REGION
$n_e(cm^{-3})$
$v\ (cm\ s^{-1})$
v_A
v
n_e
T_{eff} (K)
$T_{eff}^{Mg^{+9}}$
$T_{eff}^{Ly-\alpha}$
$T_{eff}^{O^{+5}}$
r/R_s

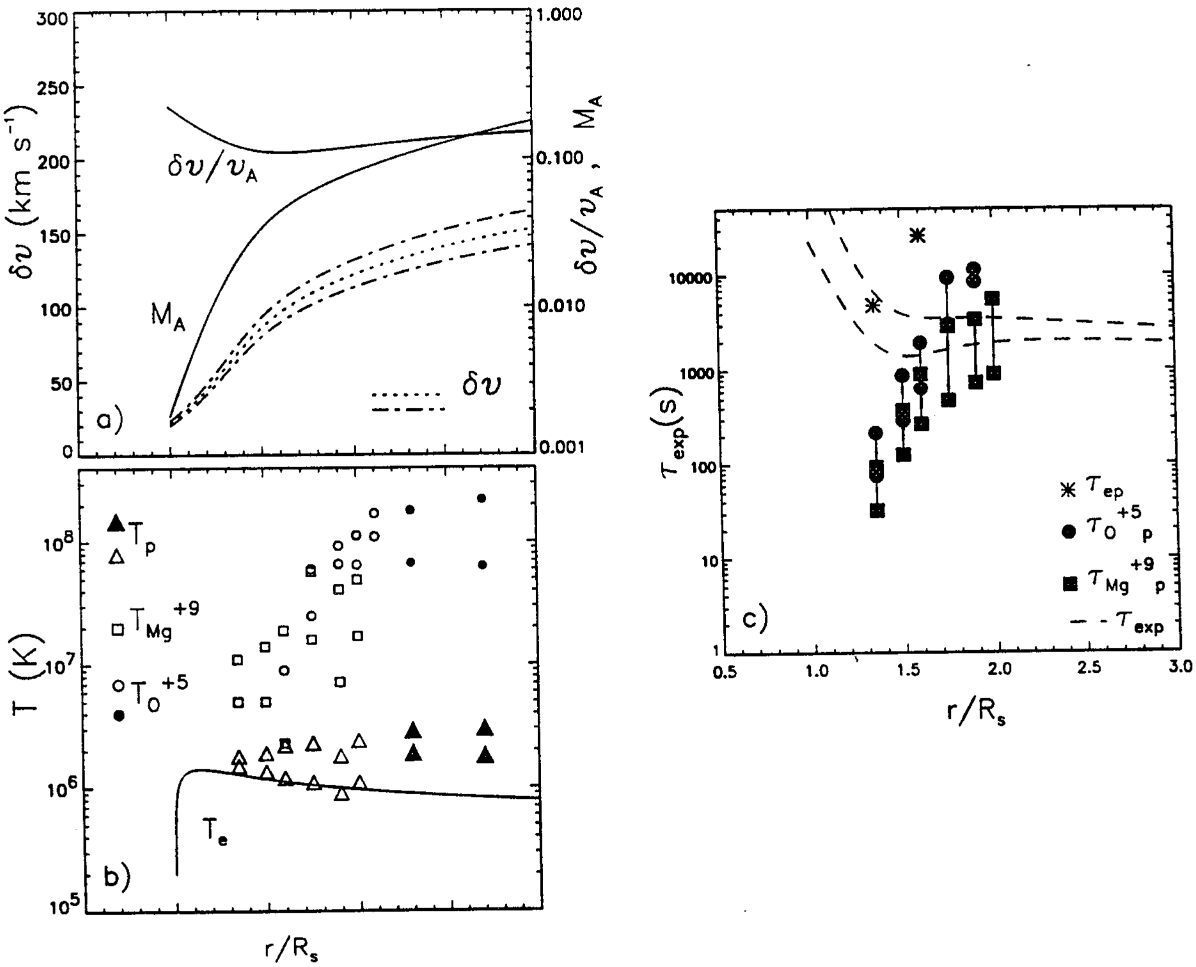

Figure 2: *a) Limits on the Alfvén wave amplitude in the coronal hole are derived from the effective temperatures of the protons and* Mg^{+9} *at 1.35* R_S *(Figure 1a) (Figure 1, lower panels) and WKB approximation (dash dotted lines), assuming that the resulting limits on* δv *have to lead to proton and magnesium temperatures with* $T_p \leq T_{Mg^{+9}}$ *at all distances. With these assumptions the limits for* δv *derived at the coronal base are* $20 \leq \delta v \leq 23$ $km\ s^{-1}$*. We compare these values to the value derived from SUMER observations, given by Tu and Marsch (1997) (see also references therein) at about 1.2* R_S*. Extrapolating their value using the WKB assumption results in* $\delta v(r)$ *(dotted line) which agrees extremely well with the limits presented here. The maximum value of the ratio* $\delta v/v_A = \delta B/B$ *is calculated from Figure 1. Alfvén waves are not damped if* $\delta v/v_A < 1$*. The ratio* $M_A = v/v_A$ *is calculated from values given in Figure 1b. b) The amplitudes in Figure 2a are used to place limits on the thermal motions for the ions. The upper and lower limits on these particle temperatures are derived from the combination of* $(T_{eff})_{\substack{max\\min}}$ *with* $(\delta v)_{\substack{min\\max}}$*. These are the ion temperatures that reflect the heating of the particles. Also shown is an electron temperature profile (solid line) derived from in situ charge state modeling (Esser et al. 1998b). c) Solar wind expansion times,* τ_{exp}*, for the electron densities shown in a and flow speed limits shown in b. Collision times for equipartition of energy between protons and the other particles,* τ_{pi}*, are calculated assuming upper values of the temperatures in a and electron densities in b (upper symbols). Minimum values (lower symbols) are calculated using average temperatures from Figure 2b.*

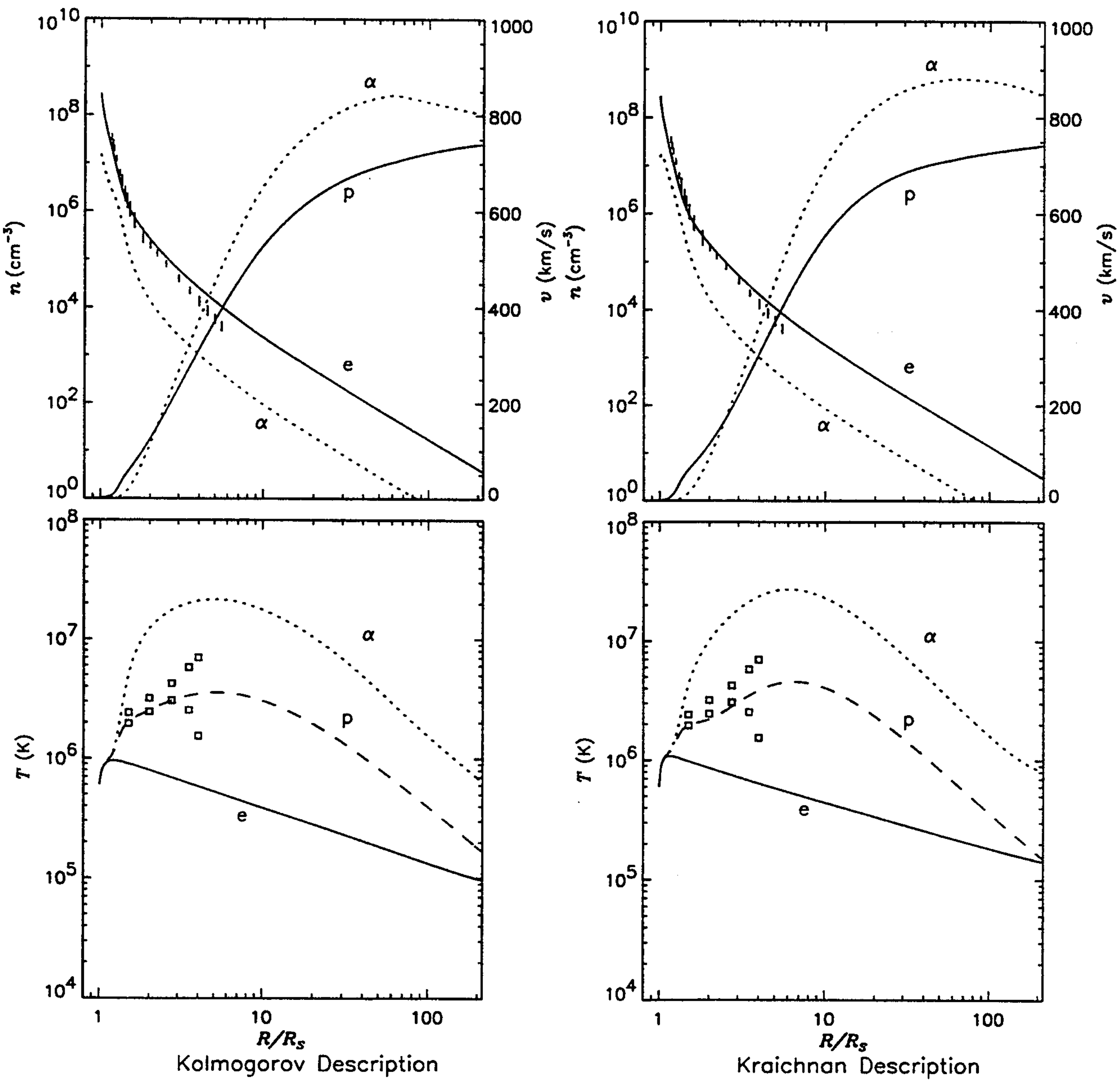

Figure 3: *Example of two different heating mechanisms which heat the solar wind ions, and UVCS spectral line observations of the Lyman-α 1215 Å line (open boxes). The temperatures derived from the models fit the observed limits, calculated flow speeds and densities are also in agreement with observational constraints. The two models give very similar results.*

1.3 Future Plans

We will continue to analyze the SOHO data, which in addition to the UVCS data also includes CDS and LASCO data. We have started to analyze the CDS coronal hole data, and expect the first results to be presented at the SW9 conference. These observations will then be integrated with the other coronal observations to gain new insight into coronal plasma conditions. We will carry out an extensive density analysis by comparing the densities derived from different techniques (line ratio and pB) and model calculations. Presently, there seem to be some inconsistencies in the electron densities derive from observations in coronal hole regions. Using both theoretical models and different types of observations, we hope to resolve these inconsistencies, and thus place more reliable constraints on the electron densities. In the studies like the ones presented above, electron densities play a crucial role, and improving their reliability, also improves the quality of other coronal constraints such as flow speeds, Doppler dimming speeds and electron temperatures derived from charge states.

New observations will in the future concentrate more on the slow solar wind. With increasing solar activity, observations of the fast solar wind will become increasingly difficult, and it seems therefore timely to move on to studying the denser coronal structures.

2. Publications in Journals and Proceedings

1. R. Esser, S. R. Habbal, W. A. Coles and J. V. Hollweg, Hot protons in the inner corona and their effect on the flow properties of the solar wind, *J. Geophys. Res.*, **102**, 7063, 1997.

2. N. S. Brickhouse, and R. Esser, Effects of High Proton Temperatures on Diagnostics for Electron Density and Electron Temperature, *Astrophys. J.*, **479**, L470, 1997.

3. X. Li, R. Esser, S. R. Habbal, and Y.-Q. Hu, Influence of Heavy Ions on the High Speed Solar Wind, *J. Geophys. Res.*, **102**, 17419, 1997.

4. R. Esser, R. J. Edgar and N. S. Brickhouse, High minor ion outflow speeds in the inner corona and observed ion charge states in interplanetary space, *Astrophys. J.*, **498**, 448, 1998.

5. Yamauchi, Y., M. Tokumaru, M. Kojima, H. Misawa, H. Mori, P. K. Manoharan, and R. Esser, Observations of micro-turbulence in the solar wind near the sun with interplanetary scintillation, *J. Geophys. Res.*, **103**, 6571, 1998.

6. R. Esser, S. Fineschi, D. Dobrzycka, S. R. Habbal, R. J. Edgar, J. C. Raymond, and J. L. Kohl, Plasma properties in coronal holes derived from measurements of minor ion spectral lines and polarized white light intensity, *Astrophys. J. Let.*, accepted 1998.